

UC San Diego

UC San Diego Previously Published Works

Title

Aqueous angiography in pre-glaucomatous and glaucomatous ADAMTS10-mutant canine eyes: A pilot study.

Permalink

<https://escholarship.org/uc/item/0m38w32v>

Journal

Veterinary Ophthalmology, 25 Suppl 1(Suppl 1)

Authors

Burn, Jessica

Huang, Alex

Weber, Arthur

et al.

Publication Date

2022-05-01

DOI

10.1111/vop.12938

Peer reviewed



Published in final edited form as:

Vet Ophthalmol. 2022 May ; 25(Suppl 1): 72–83. doi:10.1111/vop.12938.

Aqueous angiography in pre-glaucomatous and glaucomatous *ADAMTS10*-mutant canine eyes: A pilot study

Jessica B Burn¹,

Alex S Huang²,

Arthur Weber¹,

András M Komáromy¹,

Christopher G Pirie¹

¹Michigan State University

²Doheny Eye Institute, UCLA

Abstract

Objective: To evaluate intravenous scleral and intracameral aqueous angiography in normotensive (n=4) and hypertensive glaucomatous (n=6) *ADAMTS10*-mutant canine eyes.

Animals studied: Ten *ADAMTS10*-mutant dogs.

Procedures: Dogs were sedated and one eye from each dog underwent scleral angiography following intravenous injection of 0.25% indocyanine green (ICG). After a 24-hour recovery period, the same eye underwent aqueous angiography via intracameral administration of ICG. Imaging of identical scleral sectors from the same eye was performed using a Heidelberg Spectralis® Confocal Scanning Laser Ophthalmoscope. Intrasceral vessel depth and lumen diameters were measured using Heidelberg Spectralis® optical coherence tomography and computer software.

Results: Scleral angiography permitted visualization of vascular components associated with conventional aqueous humor outflow pathways with an average time from injection to fluorescence of 35.8±10.6 seconds (mean ± SD). Two normotensive eyes (2/10;20%) demonstrated turbulent dye movement, while 4 hypertensive eyes (4/10;40%) exhibited laminar flow. Aqueous angiography demonstrated dye fluorescence within the post-trabecular conventional aqueous humor outflow pathways in all 10 eyes at 34.3±11.0 seconds post-injection. Sectoral and dynamic outflow patterns were observed primarily within the superotemporal sector in 9 eyes (9/10;90%). Seven eyes (7/10;70%) demonstrated pulsatile dye movement and 5 eyes (5/10;50%) exhibited laminar flow. The degree of laminar movement of dye was greatest in hypertensive eyes. Vessel lumen diameters measured 133.85±28.36µm and 161.18±6.02µm in hypertensive and normotensive eyes, respectively.

Conclusions: Aqueous angiography allowed for visualization of fluorescent dye in the superotemporal sclera. Laminar flow and smaller lumen vessels were observed mainly in hypertensive eyes.

Keywords

canine; *ADAMTS10*; open-angle glaucoma; aqueous angiography; indocyanine green; conventional outflow

1 Introduction

Glaucoma is a common ocular disease in canines,^{1,2} with a poor prognosis for vision and long-term comfort of the eye. Disease processes such as uveitis, pupillary obstruction, a collapsed ciliary cleft and trabecular meshwork, posterior synechia, or even vitreal prolapse can potentially lead to obstruction of aqueous humor outflow and a subsequent elevation in intraocular pressure (IOP).³ While certain dog breeds are known to be at risk for developing primary glaucoma, little is known about the changes which occur within the aqueous humor outflow pathways. Furthermore, our capacity to identify “at risk” patients, prior to the onset of pressure elevations, and determine their response to current anti-glaucoma therapies is currently lacking.

Due to current diagnostic and therapeutic challenges, significant improvements in how we identify and treat dogs with glaucoma are needed. Aqueous angiography (AA), an imaging modality involving intracameral (IC) administration of a fluorescent dye, is an approach which may address some of these challenges by allowing visualization of the post-trabecular vasculature of the conventional aqueous humor outflow (CAHO) pathways.⁴⁻⁶

In canine breeds predisposed to glaucoma, for example, AA may serve as a better means to predict true “at risk” patients through demonstrating functional alterations in CAHO pathways. This could allow for earlier medical and/or surgical interventions prior to the onset of pressure elevations, which could translate into better long-term control of IOP. As primary angle-closure glaucoma (PACG) is a bilateral disease, typically affecting one eye at a time, AA has the potential to compare the CAHO pathways between eyes within the same canine: one with an elevated IOP and the other with a normal IOP. Noted differences could provide useful information, which could lead to better treatment options, such as a tailored surgical approach for gonioimplant placement in the affected eye.

Ultimately, new insights gained via AA could alter our current screening practices for evaluating predisposed breeds of dogs and those with early IOP elevations. In addition, this information could improve the current prophylactic and therapeutic medical approaches in use. AA is a unique imaging modality, which aims to bridge this knowledge gap and to improve our current understanding of glaucoma. This study aims to explore the diagnostic potential of AA in *ADAMTS10*-mutant beagles with open angle glaucoma (OAG).⁷ We hypothesize that AA will demonstrate delayed filling of CAHO pathways and/or altered outflow patterns (reduced number and caliber of post-trabecular vessels) in *ADAMTS10*-mutant dog eyes, as compared to recent observations noted in normal dog eyes, both before and after IOP increase.⁴

2 Materials and Methods

2.1 Animals and Study Design

This pilot study was designed to obtain preliminary data regarding AA in *ADAMTS10*-mutant beagle dogs, as such no power analysis and/or sample size calculations were performed. Two experiments were performed on a group of 10 purpose-bred *ADAMTS10*-mutant beagle dogs. Dogs were categorized as pre-glaucomatous, normotensive (average diurnal IOP < 20 mmHg) or glaucomatous, hypertensive (≥ 20 mmHg) with optic nerve head changes (atrophy and cupping) as documented by indirect ophthalmoscopy and optical coherence tomography over the previous 6 months. Four eyes were classified as pre-glaucomatous (mean \pm SD IOP 18.3 ± 1.5 mmHg) while 6 eyes were classified as glaucomatous (mean \pm SD IOP 27.5 ± 17.1 mmHg).

All dogs were heavily sedated and one eye from each dog was evaluated following intravenous (IV) administration (scleral angiography, SA) and subsequent IC administration (aqueous angiography, AA) of indocyanine green (ICG) after a recovery period of at least 24 hours. All dogs were deemed to be systemically healthy prior to performing AA. Indocyanine green is an unstable dye in aqueous solution and demonstrates a plasma half-life of 3–4 minutes.^{8,9} While the half-life of ICG may vary in other body tissues, a recovery period of 24 hours should permit repeated dye administration within the same dog following such a short period.

All dogs received a complete physical examination to assess general health the day prior to SA and AA being performed. Additionally, a complete ophthalmic examination, including a Schirmer tear test (Merck Animal Health: Madison, NJ, USA), topical fluorescein staining (Ful-Glo: Akorn, Decatur, IL), rebound tonometry (Tonovet, icare USA, Raleigh, NC), slit lamp biomicroscopy (Kowa SL-17; Kowa Company, Tokyo, Japan), and indirect ophthalmoscopy (Keeler All Pupil II: Keeler Instruments, Broomall, PA, USA; Pan Retinal 2.2D condensing lens; Volk Optical) was conducted. A complete ophthalmic examination was also conducted immediately after completion of angiographic studies and once daily for up to one-week post-procedure to monitor for any potential changes/complications.

All studies were performed in accordance with the ARVO Statement for the Use of Animals in Ophthalmic and Vision Research guidelines and were approved by the Michigan State University Institutional Animal Care and Use Committee.

2.2 Sedation Protocol and Surgical Preparation:

Dogs were pre-medicated with carprofen (Rimadyl; Zoetis: Parsippany, NJ) subcutaneously at 4.4 mg/kg and a standard sedation protocol was used, as previously published.¹² Briefly, for both angiographic techniques butorphanol tartrate 0.3 mg/kg intramuscular (IM) (Torbugesic; Zoetis: Parsippany, NJ) and dexmedetomidine 6mcg/kg IV (Dexdomitor, Zoetis: Parsippany, NJ) were administered. Heart rate, respiratory rate, ECG tracings, and pulse oximetry data were monitored (VM 9000; Mindray: Mahwah, NJ). Positioning of the dog and the eye to be imaged was carried out in a manner identical to that described in a recent study.⁴ Briefly, topical proparacaine hydrochloride 0.5% ophthalmic solution, USP (Akorn, Decatur, IL) was applied to the eye to be imaged for ocular surface anesthesia,

and the periocular skin and ocular surface were aseptically treated with dilute 2% povidone-iodine solution. Two stay sutures (4–0 silk; Ethicon, Somerville, NJ) were placed in the superior and inferior bulbar conjunctiva to allow for adequate globe positioning during imaging. The eyelids were manually retracted, with careful attention to avoid compression of the globe or placement of excess tension on the eyelids, to allow for adequate exposure of the sclera while imaging. Once the dogs were positioned, IOP was measured prior to and post-administration of ICG using rebound tonometry. Post-procedural rebound tonometry was performed within a timeframe of approximately 15 minutes post-injection of dye, allowing angiographic imaging to be completed without disruption.

Upon completion of angiographic imaging, a dose of 5mg/mL atipamezole (Antisedan, Zoetis: Parsippany, NJ) equivalent in volume to the dose of dexmedetomidine administered was injected IM to reverse the sedation. Neomycin-polymyxin-B-dexamethasone ophthalmic ointment (Sandoz; Princeton, NJ) was applied to the eye that was imaged on recovery and every 12 hours until resolution of any observed intraocular inflammation and/or fibrin post-imaging.

2.3 Imaging

Imaging was performed using similar methods to a previous study.⁴ A Heidelberg Spectralis® Confocal Scanning Ophthalmoscope (Heidelberg Engineering Inc.; Heidelberg, Germany), utilizing a 55° lens and automatic Real-time Tracking (ART) was employed to obtain still angiographic images and video footage of all dogs, rotating from the superior sclera through the superotemporal, temporal, and inferotemporal scleral sectors. A video sequence of the temporal region of the sclera was recorded for an initial 40 seconds immediately following injection of ICG (IV or IC). Time stamps were started post-dye injection. This sequence was repeated for a total of 10 minutes and 20 minutes following IV and IC injection of ICG, respectively.

All 10 *ADAMTS10*-mutant beagles underwent SA via IV ICG dye administration. Standard color images were taken of the superior, superotemporal, temporal, inferotemporal, and inferior scleral sectors of each eye being imaged immediately prior to angiography (Canon EOS 5D Mark IV with Canon EF 100mm f/2.8L Macro IS USM Lens, Canon, Tokyo, Japan) to demonstrate the venous circle of Hovius and to compare the same location using each imaging modality. Once the dogs were adequately sedated and positioned, 1 mg/kg ICG was administered IV through the catheter to facilitate SA. Angiography images were obtained immediately following dye administration, as described above.

AA was performed on the same eye of the same 10 *ADAMTS10*-mutant beagles, using the same sedation protocol as above, after a recovery period of at least 24 hours (mean time of 5.8 ± 1.6 days). Once the dogs were adequately sedated and positioned, a 27-gauge needle and 1 mL syringe were used to inject 0.1 mL of 0.25% ICG into the anterior chamber through the superonasal limbus. The needle was tunneled through the superonasal bulbar conjunctiva and sclera to minimize leakage of ICG post-injection and subsequent subconjunctival bleb formation. Imaging of identical scleral sectors, as performed during SA, was performed immediately following dye injection.

All intrascleral outflow channels demonstrating ICG fluorescence post-injection were subsequently imaged via optical coherence tomography (OCT) using the Heidelberg Spectralis® and an anterior segment lens to obtain cross-sectional images of the temporal aspect of the sclera. The cornea of the eye being imaged was kept moist using balanced salt solution (BSS, Alcon Laboratories Inc: Fort Worth, TX.) throughout the imaging procedure; this prevented corneal ulceration and maximized image clarity. An average of 3 cross-sectional and longitudinal scans were obtained in a rectangle centered on the scleral vessel lumen. Heidelberg Eye Explorer software (version 1.5.12.0, Heidelberg Engineering, Heidelberg, Germany) was used to view and measure the images.

Measurements and Data analysis: Measurements and data analysis were performed as published in a recent study.⁴ Briefly, upon completion of each study segment, angiogram videos were independently reviewed by 2 individuals (JB, CP) and a subjective qualitative analysis was provided for each video. The time for initial fluorescence of dye within the CAHO pathways was recorded in all eyes using descriptive statistics (means and standard deviations). The zero-time point was defined as the time of injection IV or IC. The relative absolute difference and mean value for time to fluorescence between observers were calculated. The ability to clearly visualize CAHO pathways was subjectively analyzed for both SA and AA. Characteristics of outflow pathways were recorded, including the approximate distance from the limbus, the number and caliber of outflow pathways, the presence of a circumferential vessel, and the presence of any anastomoses or complex branching pathways. Aqueous humor movements were qualified as pulsatile, turbulent, or demonstrating laminar flow.¹⁰ Pulsatile aqueous humor was observed to move in a cyclic pattern in unison with the dog's heartbeat. Turbulent flow was visualized as irregular flow of fluorescent dye as it mixed with blood upon entering the vascular channels. Laminar flow was used to describe a higher signal strength of fluorescent dye hugging the vessel wall upon entry into the blood stream. Images obtained using SA and AA in this study were compared to those from normal dogs in a recent study to evaluate for differences in characteristics of aqueous humor outflow.⁴

Digital color overlays of identical scleral sectors comparing angiographic techniques (SA vs AA) were generated using Adobe Photoshop software (Adobe, San Jose, CA) and the color range tool. Vessel luminal diameter and scleral depth were measured along the vertical axis in triplicate from cross sectional OCT images obtained, using Adobe Photoshop software and the ruler tool. A custom measurement scale was created using the scale bar generated by the Heidelberg Spectralis ® device.

Statistical analysis was performed using a paired t-test to compare baseline and post-procedure IOP results. An independent t-test was utilized to compare vessel lumen diameters between hypertensive and normotensive *ADAMTS10*-mutant dogs, and between *ADAMTS10*-mutant and wild type dogs. A one-way ANOVA and Tukey's post-hoc was utilized to compare vessel lumen diameters between wild type, normotensive *ADAMTS10*-mutant, and hypertensive *ADAMTS10*-mutant dogs. Absolute differences, individual standard deviations, and relative absolute differences were also calculated for pre- and post-procedure IOPs. Additionally, a series of chi-square tests were performed to evaluate

the presence or absence of turbulence, pulsatility, and the complexity of branching of vessels visualized between normotensive and hypertensive eyes.

3 Results

3.1 Intravenous (IV) Scleral Angiography (SA):

All 10 eyes had mean immediate pre- and post-procedure IOP values of 23.2 ± 10.4 mmHg and 17.1 ± 8.6 mmHg, respectively. These values varied slightly from the baseline measurements with 5 eyes exhibiting pre-SA IOP ≥ 20 mmHg (range 20.0–43.0 mmHg) and 5 eyes demonstrating pre-SA IOP < 20 mmHg (range 7.0–19.0 mmHg). There was no statistically significant difference between the pre- and post-SA IOP values when compared using a paired t-test ($\alpha = 0.05$, p-value = 0.17) (Table 1).

The sedation protocol employed, in combination with topical anesthesia and suture placement, allowed SA to be readily performed. Imaging of the left eye was randomly selected for the first 5 dogs, and the right eye was assigned to 4 dogs. The remaining eye was assigned to the left eye due to the right eye being used in a separate study. No eye imaged was receiving any topical therapy at the time of angiography.

For each eye, an average of 6.7 still images and 4.3 video clips were obtained following the initial 40 second video sequence. Progressive filling of conjunctival vessels followed by intrascleral vessels were clearly visualized in all 10 eyes, with an average initial onset of filling time occurring at 35.8 ± 10.6 seconds. The mean absolute difference between the two graders was 0.80 seconds, while the mean individual standard deviation was 0.92 seconds.

Complex, branching patterns with multiple anastomoses involving the scleral, episcleral, and conjunctival vasculature was observed post-injection. Clear visualization of deep intrascleral vessels, consistent with the circle of Hovius, was observed within the temporal (10/10), superotemporal (6/10), superior (1/10), and inferotemporal (1/10) scleral sectors. Of the 6 eyes classified as hypertensive, 2/6 demonstrated no movement of dye once filling of the deep scleral vessels were complete while 4/6 demonstrated visualization of laminar flow. One of the 2 eyes which demonstrated no movement of dye also showed markedly delayed filling (Dog 4). The remaining 4 normotensive eyes, with baseline IOPs within the normal range demonstrated turbulent dye movement within the deep scleral vessels during the filling phase (2/4), laminar flow (1/4), and lack of dye movement (1/4). Turbulent flow was visible as irregular fluctuations, both in the speed and direction of dye movement, upon mixture with blood in vessel lumens (Video 1) Upon complete filling of all luminal vessels, no variation of the fluorescent signal intensity was observed during the remainder of the imaging time period.

3.2 Intracameral (IC) Aqueous Angiography (AA):

No eyes demonstrated evidence of residual ICG fluorescence from recent SA. The mean IOP measured pre- and post-ICG administration of all 10 eyes imaged were 22.7 ± 5.6 mm Hg and 10.5 ± 8.5 mm Hg, respectively. Immediate pre-procedure IOP was measured to be ≥ 20 mmHg in 5 eyes (range 21.0–35.0 mmHg), and < 20 mmHg in 5 eyes (range 18.0–19.0 mmHg). A clinically significant difference was observed between pre- and post-IOP results

of all eyes when compared using a paired t-test ($\alpha = 0.05$, $p\text{-value} = 0.001$). Individual pre- and post-procedure IOP results, including their absolute differences, individual standard deviations, and relative absolute differences are listed in Table 2.

An average of 5.4 still images and 11.2 video clips after the initial 40 second video sequence were captured for each eye. Diffuse and uniform fluorescence of ICG within the anterior chamber was visualized in all eyes, immediately following IC injection. The average time to observe initial dye fluorescence within an intrascleral channel(s) was 34.3 ± 11.0 seconds post injection. The mean absolute difference between the two graders was 0.9 seconds, while the mean individual standard deviation as 1.29 seconds. All 10 eyes imaged demonstrated dye fluorescence within various scleral sectors. Fluorescence was visualized within the superotemporal sclera, displaying complex intra-scleral branching patterns in 9/10 eyes (90%). One eye from Dog 8 demonstrated fluorescence in the temporal scleral sector only. Initial fluorescence typically occurred within a large deep intrascleral vessel and rapidly progressed into numerous complex branching intrascleral luminal vessels. The subjective intensity of fluorescence within these intrascleral vessels was progressive over time, particularly as dye flowed into neighboring intrascleral and conjunctival draining pathways. (Fig 1) One eye imaged from Dog 9 demonstrated subsequent fluorescence within 3 solitary conjunctival vessels located in the superior scleral sector, after initial filling and dye fluorescence within neighboring deeper intrascleral vessels. Pulsatility of dye was visualized in 7/10 eyes imaged and was noted to occur primarily within larger intrascleral vessels as dye movement progressed into the superficial vasculature, the frequency of which appeared to align with the dog's heart rate. (Video 1 and 2) Of the 7 eyes demonstrating pulsation, 2 eyes were classified as exhibiting moderate pulsation (1 hypertensive and 1 normotensive eye), while the remaining 5 eyes exhibited mild pulsation (3 hypertensive and 2 normotensive eyes). Laminar flow was observed in a total of 5/10 eyes (4 hypertensive and 1 normotensive eye). In 3/10 eyes, no pulsatility or laminar flow was observed (2 hypertensive and 1 normotensive eyes). One of the hypertensive dogs exhibiting a lack of pulsatility or laminar flow also exhibited marked delayed filling during both AA and SA (Dog 4).

3.3 Comparison of Intracameral (IC) and Intravenous (IV) Routes of Injection:

Representative color, AA and SA images (Fig 2), depicting identical scleral sectors, illustrate consistencies between the two angiographic techniques. Both angiographic modalities permitted visualization of luminal vessels within the sclera in most dogs, consistent with the intrascleral venous plexus and the venous circle of Hovius. AA highlighted movement of dye from within the anterior chamber into the vascular components affiliated with the CAHO (intrascleral plexus and circle of Hovius). While SA routinely permitted visualization of similar vasculature components of the CAHO, this modality also highlighted the more superficial episcleral and conjunctival vasculature.

Intrascleral vessels were variable both in their luminal diameter and location within the sclera. (Fig 3) Vessel luminal diameters ranged from $91.75 \mu\text{m}$ to $157.81 \mu\text{m}$ (mean \pm SD $138.54 \pm 23.70 \mu\text{m}$) and $91.75 \mu\text{m}$ to $173.71 \mu\text{m}$ (mean \pm SD $144.78 \pm 27.41 \mu\text{m}$) during SA and AA, respectively. Although no statistically significant difference in vessel

lumen diameter between hypertensive (SA; $129.19 \pm 23.4 \mu\text{m}$, AA; $133.85 \pm 28.36 \mu\text{m}$) and normotensive eyes (SA; $154.14 \pm 3.00 \mu\text{m}$, AA; $161.18 \pm 6.02 \mu\text{m}$) was observed during SA or AA ($\alpha=0.05$, $P=0.1$ and $P=0.08$), a trend towards a smaller vessel diameter in eyes with increased IOPs was noted. Additionally, the smallest lumen diameter was noted in a hypertensive eye with the highest recorded IOP (Dog 4). Similar measurements obtained from wild-type dogs in a recent study reported a mean \pm SD vessel lumen diameter of $258.0 \pm 9.1 \mu\text{m}$.¹¹ (Fig 4) An independent t-test was used to compare the caliber of vessel size measured from AA imaging in eyes of *ADAMTS10*-mutant dogs as compared to eyes from unaffected normal dogs¹² and a statistically significant difference was found ($\alpha=0.05$, $p=0.00039$). A one-way between groups ANOVA comparing luminal diameter between unaffected wild-type normal, pre-glaucomatous *ADAMTS10*-mutant, and glaucomatous *ADAMTS10*-mutant dogs from AA imaging demonstrated statistical significance [$F(2,15) = 9.1$, $p=0.0019$]. A Tukey post-hoc test showed that pre-glaucomatous *ADAMTS10*-mutant dogs and glaucomatous *ADAMTS10*-mutant dogs were significantly different from unaffected normal dogs at a $p < 0.05$ but were not significantly different from each other. Vessel depth within the mid-to-deep stromal tissue was not statistically significant when comparing hypertensive and normotensive eyes using AA ($\alpha=0.05$, $P=0.9$); or SA ($\alpha=0.05$, $P=0.39$).

No statistically significant difference was observed when assessing the presence or absence of turbulence, pulsatility, and/or the complexity of branching of vessels visualized between normotensive and hypertensive eyes.

A multipartite stratification pattern of laminar flow was seen with AA, but not SA. With AA, increasing intensity of dye towards the periphery of the vessel could be seen in dogs with laminar flow (Fig 5, Video 2) Of the 5 eyes exhibiting laminar flow during AA, 4 eyes exhibited an elevated IOP, while 1 eye had a measured baseline and immediate pre-procedure IOP < 20.0 mmHg.

3.4 Safety:

No complications were observed with the sedation protocol employed to conduct these angiographic techniques in any of the dogs. However, minor complications associated with SA and AA were observed. All dogs demonstrated mild aqueous flare the day following the procedure (1+ flare using the SUN scale)¹². These clinically detectable signs of intraocular inflammation resolved 24 hours and 48 hours following SA and AA, respectively. A small fibrin tag was visualized in 2 eyes, following AA, which resolved with ongoing topical anti-inflammatory treatment for 10 days.

4 Discussion

This pilot study demonstrates the use of AA and provides insight into the CAHO pathways of *ADAMTS10*-mutant dogs. In the current study, complex branching patterns seen with AA in both normotensive and hypertensive *ADAMTS10* were largely restricted to the temporal and superotemporal sclera. These findings are in alignment with *ex vivo* studies evaluating a subset of glaucomatous eyes from dogs and cats.^{5,10, 13} However, in normal dogs, a greater variation in the location of dye fluorescence was observed.⁴ The noted restriction as to

where dye visualization was observed in *ADAMTS10*-mutant dogs could have resulted from a change driven by IOP elevations or morphologic changes to the outflow pathways as a result of the disease process itself. Two of the three eyes in which no distinct visualization of dye movement (pulsation) within the scleral vasculature was observed were hypertensive (baseline IOP 26.0; Dog 5 and 39.3 mmHg; Dog 4). The one remaining eye was from a normotensive dog (baseline IOP of 16.3 mmHg; Dog 9). Although the underlying reason for these differences in visualization of dye and the effect of IOP remains unknown, it is speculated that the variations observed between hypertensive and normotensive *ADAMTS10*-mutant eyes may be attributed to subtle decreases in conventional aqueous humor outflow as IOP begins to rise. It is also plausible that intermittent spikes in IOP could have been occurring between IOP measurements, such that they were not detected at the time of measurement.

In this study, pulsatile movement of ICG dye was a frequent observation within intrascleral vessels of *ADAMTS10*-mutant eyes (7/10; 70% eyes) imaged with AA, as compared to a previous study of normal dogs (4/12; 33%).⁴ (Video2) This observation, given 4/7 eyes were hypertensive, could be the direct effect of increasing IOP, creating a surge to drive the choroid piston effect.¹⁴ The end result generating more prominent pulsatile movement of dye within the outflow vascular channels. Increased dye pulsation, as noted herein, may alternatively reflect structural alterations to the scleral biomechanics and/or to the CAHO pathways already in place, given the animal model being used. It has been shown that *ADAMTS10*-OAG dogs have lower dynamic and viscoelastic posterior scleral properties and less insoluble collagen compared to age-matched control dogs.¹⁵ A weaker sclera in affected dogs could explain the increased visualization of dynamic movement, such as pulsatility of dye in the intrascleral vessels, due to decreased resistance of the scleral tissue.¹⁵ Alternatively, increased resistance to blood flow, relating to alterations in scleral compliance or vessel luminal diameter, could account for these observations. Finally, this dynamic movement could also be due to altered states in blood pressure and its impact on ocular perfusion pressure, as seen in humans with open angle glaucoma.¹⁶ Systemic blood pressure was not measured in this study, but is measured regularly in this group of dogs, and no indication of systemic hypertension has been noted. Despite this, it is plausible that ocular perfusion could be reduced with systemic hypertension and this could occur even before elevations in IOP are detected. In the current study, laminar flow within the intrascleral vessels was also a common observation, being noted in a total of 5 eyes (4 hypertensive, 1 normotensive eye), all of which demonstrated pulsatility during AA. While laminar flow was readily visualized following AA, its presence was further highlighted using digital overlays, comparing AA vs SA. Use of the color overlays aided in demonstrating the presence of a thin column of ICG fluorescence immediately adjacent to the vessel wall (Fig 5). Although this approach did not help with measuring signal intensity, the use of digital color overlays may be useful in delineating laminar flow and its characteristics in future studies. When compared to normal eyes from a recent study, eyes from *ADAMTS10*-mutant dogs subjectively demonstrated less pronounced lamination within vessel lumens.⁴ This observation could simply be explained by a decreased volume of aqueous humor outflow. Alternatively, this may reflect a reduction in the luminal size of intrascleral vessels in glaucomatous eyes. In this study, a statistically significant difference

was found between the vessel size measured from AA imaging in eyes of *ADAMTS10*-mutant dogs as compared to eyes from unaffected normal dogs. However, no statistical significance was observed in vessel lumen diameter between hypertensive and normotensive eyes. Despite this, a clinically relevant trend was noted wherein smaller vessel diameters were seen in eyes with elevated IOPs; the smallest lumen diameter measured was in a hypertensive eye with the highest recorded IOP in the study (Dog 4). There are potential shortcomings with measuring vessel lumen diameter using OCT. The authors aimed to mitigate these shortcomings by obtaining OCT images in a plane as perpendicular as possible to the vessel of interest and by taking measurements in triplicate. However, it is still possible that a slightly oblique angle of the vessel could have been imaged and subsequently measured, leading to falsely elevated vessel lumen diameters.

There is currently limited data regarding the caliber of scleral vessels observed *in vivo*, and the onset of dye filling and/or the time to complete dye filling within CAHO pathways of normal dog eyes. Overall, relatively more eyes in this study with an elevated IOP had visible turbulent and/or pulsatile flow of aqueous humor when AA was performed as compared to normal dogs.¹¹ Despite this finding, there was no statistically significant association between vessel lumen diameter and IOP values. However, a noticeable trend was observed with eyes having higher IOPs also having smaller vessel lumen diameters. The small sample size as well as variations in the regional outflow of fluorescent dye, similar to the differences in regional outflow observed in human eyes, may account for the lack of statistical significance in this pilot study.¹⁷

The trending but not statistically significant differences comparing the outflow of normal to glaucoma dogs has multiple possible explanations. First, this pilot study was of limited sample size, and additional statistical power may have been necessary. Making comparisons between normal to glaucoma dogs with higher IOP elevations, then those reported herein, would have likely improved our ability to detect significant differences should they exist. Then technical aspects must be considered. It is possible that changes in pressure or obstruction of aqueous outflow as a result of manual eyelid retraction or the use of conjunctival stay sutures were confounders. Lastly, a gravity-fed constant pressure tracer delivery system would have been ideal, permitting direct regulation of IOP. This has been reported in post-mortem pig¹⁸, cat⁵, cow¹⁹, and human²⁰ eyes. Additionally, we have reported on this for post-mortem dog eyes⁴. For living subjects, this has been reported in live non-human primate²¹ and human eyes.^{17, 22, 23} However, we could not replicate use of a gravity-fed constant pressure tracer delivery system in living dogs and as such, we undertook an alternative injection method, as recently reported.⁴ This minimally invasive approach is arguably more clinically relevant as most clinicians would prefer to inject tracer and avoid complicated perfusion apparatuses. However, a disadvantage is IOP may become transiently high upon injection, the results of which, could impact aqueous humor outflow characteristics and AA. Ultimately, future studies evaluating injection techniques and their true impact on IOP and AA are necessary. Overall, AA (and SA) may have application in the future in dogs to identify the threshold of IOP at which physiologic changes are seen with regards to aqueous humor outflow. This may help to tailor treatments to preserve vision in different forms of canine glaucoma. Thus, AA could be used to detect early functional

abnormalities and to implement patient-specific treatment approaches as it allows for the identification and functional characterization of the CAHO pathways *in vivo*.

Conclusion

This study demonstrates the use of AA and provides baseline data regarding the CAHO pathways in *ADAMTS10*-mutant dogs. All eyes imaged in this study demonstrated visible aqueous humor outflow primarily within the superotemporal scleral sector. Pulsatility was observed in a similar number of hypertensive (4/7) and normotensive eyes (3/7), while laminar flow was observed mainly in hypertensive eyes (4/5). A trend towards smaller vessel lumen diameters was observed in hypertensive eyes compared to normotensive eyes from *ADAMTS10*-mutant dogs.

Supplementary Material

Refer to Web version on PubMed Central for supplementary material.

Acknowledgements

We thank MSU Campus Animal Resources for their technical assistance. We also thank Dr. Gillian J. McLellan at the University of Wisconsin for her assistance with troubleshooting AA techniques, and Dr. Laurence Occelli for her assistance with imaging technique and data management.

Funding Sources:

Michigan State University College of Veterinary Medicine Endowed Research Funds

Michigan State University startup funds

NIH grant R01-EY025752, Bright Focus Foundation

NIH R01EY030501

Research to Prevent Blindness Unrestricted Grant to UCLA

References

1. Gelatt KN, Mackay EO. Secondary glaucomas in the dog in North America. *Vet Ophthalmol.* 2004;7(4):245–259. [PubMed: 15200621]
2. Gelatt KN, Mackay EO. Prevalence of the breed-related glaucomas in pure-bred dogs in North America. *Vet Ophthalmol.* 2004;7(2):97–111. [PubMed: 14982589]
3. Alm A, Nilsson SFE. Uveoscleral outflow - A review. *Exp Eye Res.* 2009;88(4):760–768. [PubMed: 19150349]
4. Burn JB, Huang AS, Weber AJ, Komáromy AM, Pirie CG. Aqueous angiography in normal canine eyes. *Transl Vis Sci Technol.* 2020;9(9):1–17. doi:10.1167/tvst.9.9.44
5. Snyder KC, Oikawa K, Williams J, et al. Imaging distal aqueous outflow pathways in a spontaneous model of congenital glaucoma. *Transl Vis Sci Technol.* 2019;8(5):22.
6. McLellan GJ, Snyder KC, Oikaw K, Kiland JA, Gehrke S, Huang AS. Imaging distal aqueous outflow pathways in a spontaneous model of primary congenital glaucoma (PCG). *Invest Ophthalmol Vis Sci.* 2018;59:5908.
7. Kuchtey J, Olson LM, Rinkoski T, et al. Mapping of the disease locus and identification of *ADAMTS10* as a candidate gene in a canine model of primary open angle glaucoma. *PLoS Genet.* 2011;7(2):e1001306. doi:10.1371/journal.pgen.1001306 [PubMed: 21379321]

8. Meijer DKF, Weert B, Vermeer GA. Pharmacokinetics of biliary excretion in man. VI. Indocyanine green. *Eur J Clin Pharmacol.* 1988;35:295–303. [PubMed: 3181282]
9. Ott P, Keidin S, Johnsen AH, Bass L. Hepatic removal of two fractions of indocyanine green after bolus injection in anesthetized pigs. *Am J Physiol.* 1994;266(6):1108–1122.
10. Johnstone M, Martin E, Jamil A. Pulsatile flow into the aqueous veins: Manifestations in normal and glaucomatous eyes. *Exp Eye Res.* 2011;92(5):318–327. [PubMed: 21440541]
11. Burn JB, Huang AS, Weber AJ, Komáromy AM, Pirie CG. Aqueous angiography in normal canine eyes. In: American College of Veterinary Ophthalmology; November 6–November 9, 2019; Maui, HI, Abstract G50.
12. Trusko B, Thorne J, Jabs D, et al. The standardization of uveitis nomenclature (SUN) project: Development of a clinical evidence base utilizing informatics tools and techniques. *Methods Inf Med.* 2013;52(3):259–265. doi:10.3414/ME12-01-0063 [PubMed: 23392263]
13. Telle MR, Snyder KC, Teixeira LBC, et al. Development and validation of new methods to visualize conventional aqueous outflow pathways in canine glaucoma. In: American College of Veterinary Ophthalmologists 49th Annual Conference, Minneapolis MN, September 26–29, 2018. ; 2018.
14. Phillips C, Tsukahara S, Hosaka O, Adams W. Ocular pulsation correlates with ocular tension: the choroid as piston for an aqueous pump? *Ophthalm Res.* 1992;24:338–343.
15. Palko JR, Iwabe S, Pan X, Agarwal G, Komáromy AM, Liu J. Biomechanical properties and correlation with collagen solubility profile in the posterior sclera of canine eyes with an ADAMTS10 mutation. *Invest Ophthalmol Vis Sci.* 2013;54(4):2685–2695. [PubMed: 23518772]
16. Cantor E, Méndez F, Rivera C, Castillo A, Martínez-Blanco A. Blood pressure, ocular perfusion pressure and open-angle glaucoma in patients with systemic hypertension. *Clin Ophthalmol.* 2018;12:1511–1517. [PubMed: 30197496]
17. Huang AS, Penteadó RC, Saha SK, et al. Fluorescein aqueous angiography in live normal human eyes. *J Glaucoma.* 2018;27(11):957–964. [PubMed: 30095604]
18. Saraswathy S, Tan JCH, Yu F, et al. Aqueous Angiography: Real-Time and Physiologic Aqueous Humor Outflow Imaging. *PLoS One.* 2016;11(1):e0147176. doi:10.1371/journal.pone.0147176 [PubMed: 26807586]
19. Huang AS, Saraswathy S, Dastiridou A, et al. Aqueous angiography with fluorescein and indocyanine green in bovine eyes. *Transl Vis Sci Technol.* 2016;5(6):5.
20. Huang AS, Saraswathy S, Dastiridou A, et al. Aqueous angiography–mediated guidance of trabecular bypass improves angiographic outflow in human enucleated eyes. *Invest Ophthalmol Vis Sci.* 2016;57(11):4558–4565. [PubMed: 27588614]
21. Huang AS, Li M, Yang D, Wang H, Wang N, Weinreb RN. Aqueous angiography in living nonhuman primates shows segmental , pulsatile , and dynamic angiographic aqueous humor outflow. *Ophthalmology.* 2017;124(6):793–803. [PubMed: 28237425]
22. Huang AS, Camp A, Xu BY, Penteadó RC, Weinreb RN. Aqueous Angiography: Aqueous Humor Outflow Imaging in Live Human Subjects. *Ophthalmology.* 2017;124(8):1249–1251. [PubMed: 28461013]
23. Huang AS, Penteadó RC, Papoyan V, Voskanyan L, Weinreb RN. Aqueous angiographic outflow improvement after trabecular microbypass in glaucoma patients. *Ophthalmol Glaucoma.* 2019;2(1):11–21. [PubMed: 31595267]

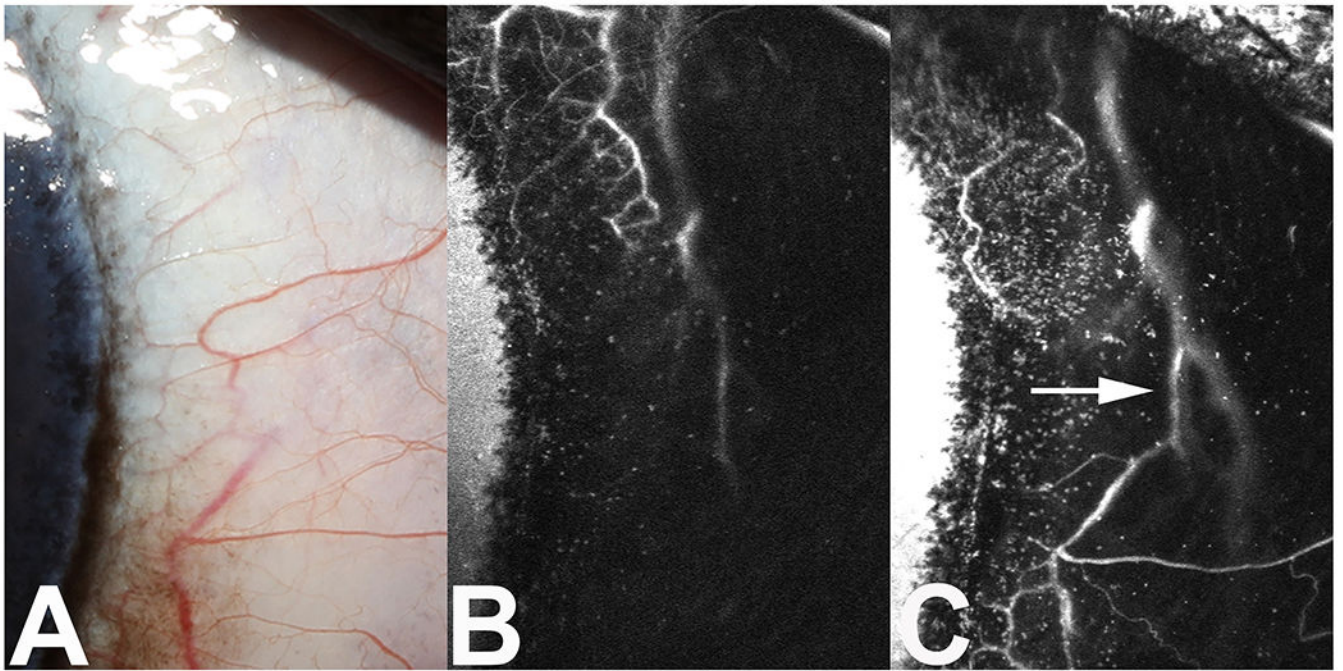


Figure 1. Standard color image of the temporal sclera of the left eye (A), aqueous angiography of the same area showing the appearance of 0.25% ICG dye fluorescence initially (B) and 20 minutes after IC injection (C), demonstrating progression of dye fluorescence and the presence of laminar flow (arrow) within the scleral vessel over time in a 4-year-old glaucomatous female beagle dog (Dog 3, baseline IOP 27 mmHg).

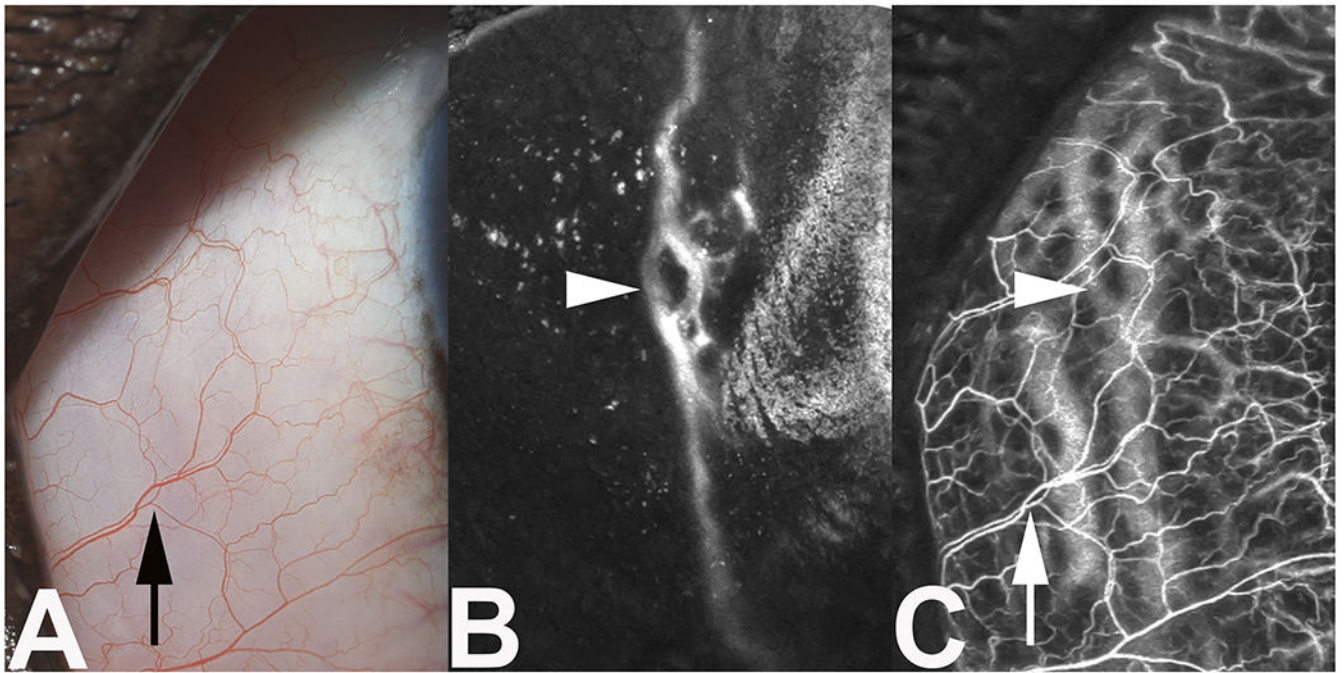


Figure 2. Comparison of different imaging techniques (standard color, AA, SA) performed in the temporal sclera in a 1-year-old normotensive *ADAMTS10*-mutant male beagle dog (Dog 7, baseline IOP 19 mmHg). Standard color image of the temporal sclera in a showing branching of conjunctival vessels (black arrow) (A). Imaging of the same location after IC injection of 0.25% ICG dye yields fluorescence of a deep scleral vessel (B). Scleral angiography, using 1 mg/kg ICG, of the same region confirms the presence of the same deep scleral vessel (arrowhead), along with numerous thinner, branching conjunctival vessels (white arrow; same vessel as depicted in (A) (C).

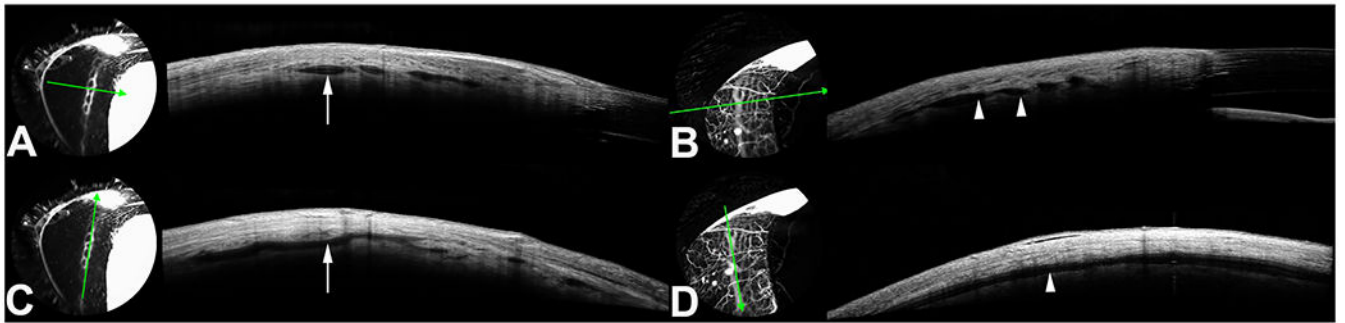


Figure 3.

OCT imaging was performed in conjunction with aqueous angiography (A, C) and scleral angiography (B, D) in the left eye of a 1-year-old normotensive *ADAMTS10*-mutant female beagle dog (Dog 6, baseline IOP 19.7 mmHg). Cross-sectional scans (A, B) and longitudinal scans of the scleral tissue (C, D) were performed. The orientation of each scan is indicated by the direction of the green arrows. The presence of scleral vessels in the mid-to-deep stromal tissue were seen in cross section (single arrow, double arrowhead) (A, B) and in longitudinal section (single arrow, single arrowhead) (C, D). Measurements of the vessels were taken through the vertical axis of each vessel lumen, using computer software.

Vessel Lumen Diameter and Depth in Unaffected Wild-type, Normotensive ADAMTS-10, and Hypertensive ADAMTS-10 mutant dogs

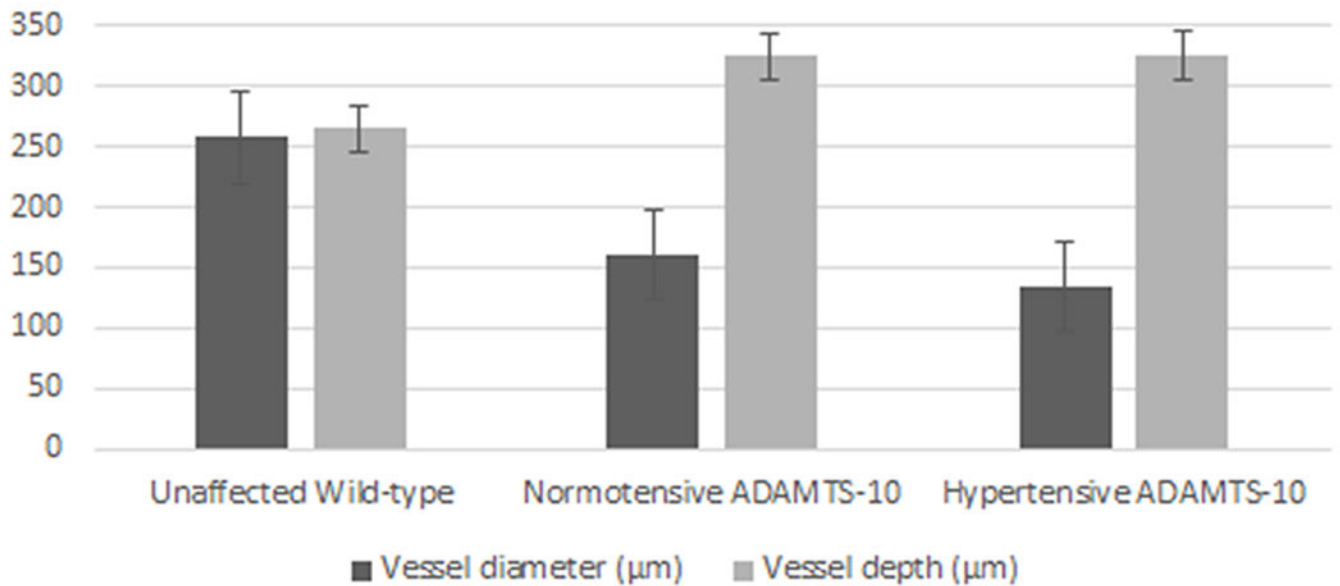


Figure 4.

Bar graph demonstrating vessel lumen diameters (μm) and scleral depth (μm) measured during AA in 12 unaffected wild-type dogs, 4 normotensive and 6 hypertensive *ADAMTS10*-mutant dogs. A reduction in vessel lumen diameter is seen in *ADAMTS-10* dogs, which is greater in hypertensive dogs, as compared to wild-type dogs.

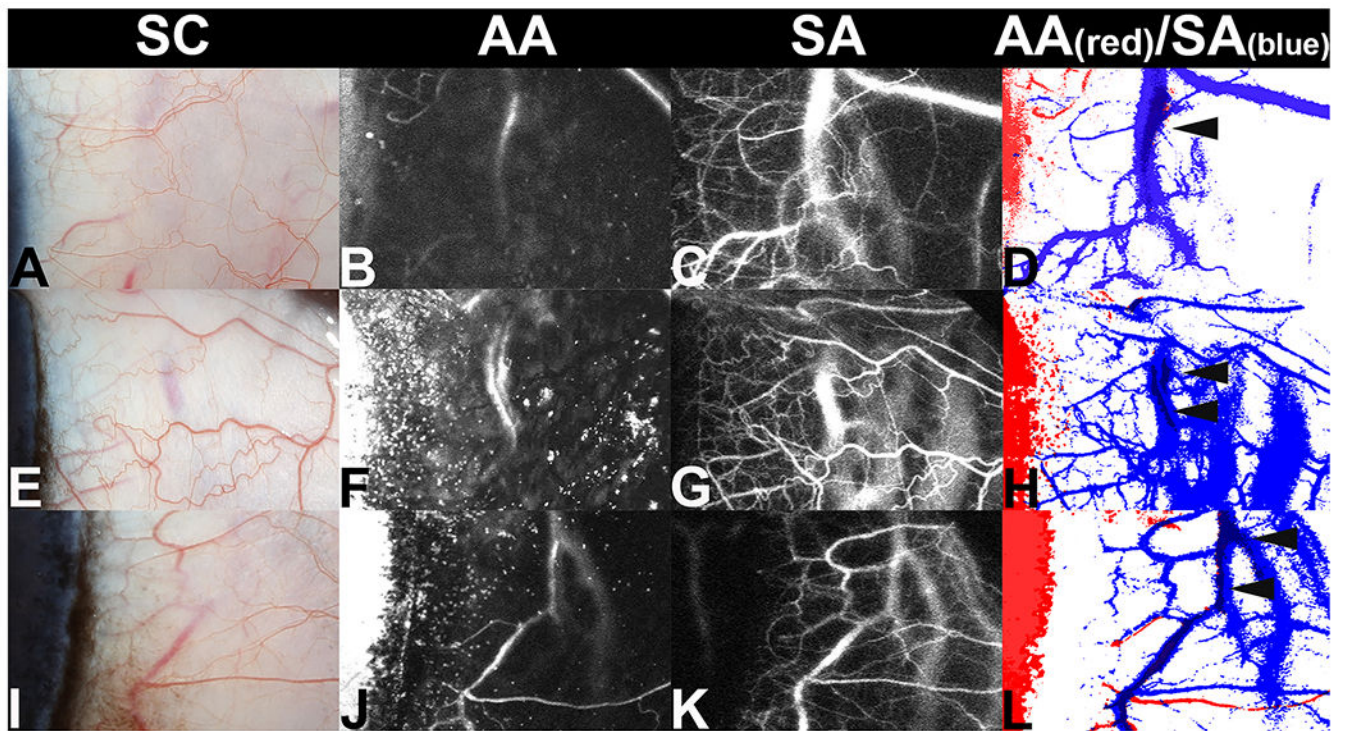


Figure 5. Standard color (SC) images of the temporal sclera of the left eye in 3 different hypertensive *ADAMTS10*-mutant beagle dogs: a 4-year-old male (Dog 1, baseline IOP 20 mmHg) (A), a 4-year-old male (Dog 2, baseline IOP 31 mmHg) (E), and a 4-year-old female (Dog 3, baseline IOP 27 mmHg) (I) with fluorescence of ICG dye in the deep scleral vessels following aqueous angiography (AA; B, F, J, respectively) and scleral angiography (SA; C, G, K, respectively). Scleral angiography demonstrates the presence of a complex branching pattern of deep scleral vessels, with thinner, superficial conjunctival vessels in the overlying tissue. Color maps were made to show simultaneous SA and AA results for each *ADAMTS10*-mutant dog (D, H, L); AA highlights ICG fluorescent patterns in red, while SA is depicted in blue.

Table 1: Summary of *ADAMTS10*-mutant dogs utilized for conducting scleral angiography (SA)

ID	Sex	Age (years)	Body Weight (kg)	Eye	Vessel Lumen Diameter (µm)	Vessel Lumen Depth in Sclera (µm)	Laminar and Bi-Directional Flow within Circle of Hovius	Baseline IOP (mmHg)	Pre-Experiment IOP (mm Hg)	Post-Experiment IOP (mm Hg)	Change in IOP	Absolute difference (A vs B)	Individual SD (A vs B)	Relative % difference (A vs B)
1	M	4.00	14.00	OS	-	-	Laminar flow	20.0	23	15	↓	8	5.66	32.10(↓)
2	M	4.00	13.00	OS	146.80	349.87	Laminar flow	31.3	31	32	↑	1	0.71	3.17(↑)
3	F	4.00	11.50	OS	137.63	352.32	Laminar flow	27.3	34	25	↓	9	6.36	30.51(↓)
4	M	3.00	15.00	OS	91.75	289.93	None	39.3	43	26	↓	17	12.02	49.27(↓)
5	F	3.00	9.65	OS	113.77	333.97	None	26.0	20	15	↓	5	3.54	28.57(↓)
6	F	1.00	9.55	OD	154.14	275.25	Bi-directional flow	19.7	16	9	↓	7	4.95	56.00(↓)
7	M	1.00	10.60	OD	-	-	Laminar flow	19.0	19	12	↓	7	5.95	45.16(↓)
8	M	1.00	14.30	OD	150.47	326.63	Bi-directional and laminar flow	18.1	23	20	↓	3	2.12	13.95(↓)
9	M	1.00	15.00	OD	157.81	300.94	None	16.3	7	4	↓	3	2.12	54.55(↓)
10	F	3.00	9.70	OS	155.98	306.45	Laminar flow	21.3	16	13	↓	3	2.12	20.69(↓)
Mean		2.5	12.2		138.54	316.92		23.8	23.2	17.1		6.3	4.45	34.40
SD		1.4	2.3		5.63	7.59		7.2	10.4	8.6		4.57	3.23	17.95

Note: Baseline IOP values over 6 months prior to the start of the study were calculated as a mean

M, male; F, female; OD, right eye; OS, left eye; Absolute difference = |A-B|; Individual SD = [(A-B)/2]/2]; Relative absolute difference (given a % change) = |A-B|/[(A+B)/2]; A=pre IOP; B=post IOP

Table 2:Summary of *ADAMTS10*-mutant dogs utilized for conducting aqueous angiography (AA)

ID	Eye	Vessel Location	Vessel Lumen Diameter (µm)	Vessel Lumen Depth in Sclera (µm)	Vessel Complexity and Pulsation	Baseline IOP (mmHg)	A (mm Hg)	B (mm Hg)	Change in IOP	Absolute Difference (A vs B)	Individual SD (A vs B)	Relative % difference (A vs B)
1	OS	Superotemporal	173.71	349.87	Complex, bifurcations, mild pulsation, laminar flow	20.0	18	7	↓	11	7.78	88.00(↓)
2	OS	Superotemporal	148.64	348.65	Complex, bifurcations, moderate pulsation, laminar flow	31.3	28	9	↓	19	13.44	102.70(↓)
3	OS	Superotemporal	135.79	313.79	Complex, bifurcations, mild pulsation, laminar flow	27.3	19	5	↓	14	9.90	116.67(↓)
4	OS	Superotemporal	91.75	289.93	Complex, bifurcations, no pulsation	39.3	35	33	↓	2	1.41	5.88(↓)
5	OS	Superotemporal	102.76	350.49	Complex, bifurcations, slow filling with no pulsation	26.0	21	3	↓	18	12.72	150.00(↓)
6	OD	Superotemporal	165.15	385.35	Complex, bifurcations, mild pulsation	19.7	18	13	↓	5	3.54	32.26(↓)
7	OD	Superotemporal	156.59	330.30	Complex, bifurcations, moderate pulsation, laminar flow	19.0	27	10	↓	17	12.02	91.89(↓)
8	OD	Superotemporal	168.82	269.13	Single vessel, weak progression, mild pulsation	18.1	19	5	↓	14	9.90	116.67(↓)
9	OD	Superior	154.14	313.79	Three vessels with little branching, no pulsation	16.3	19	10	↓	9	6.36	62.07(↓)
10	OS	Superotemporal	150.47	300.94	Complex bifurcations, weak progressive filling, mild pulsation	21.3	23	10	↓	13	9.19	78.79(↓)
Mean			144.78	325.22		23.8	22.7	10.5		12.2	8.27	84.49

ID	Eye	Vessel Location	Vessel Lumen Diameter (µm)	Vessel Lumen Depth in Sclera (µm)	Vessel Complexity and Pulsation	Baseline IOP (mmHg)	A (mm Hg)	B (mm Hg)	Change in IOP	Absolute Difference (A vs B)	Individual SD (A vs B)	Relative % difference (A vs B)
SD			5.70	6.43		7.2	5.6	8.5		5.55	3.93	42.43

Note: Baseline IOP values over 6 months prior to the start of the study were calculated as a mean

OD, right eye; OS, left eye; Absolute difference = $|A-B|$; Individual SD = $[(A-B)^2]/2$; Relative absolute difference (given a % change) = $|A-B|/[(A+B)/2]$; A=pre IOP, B=post IOP